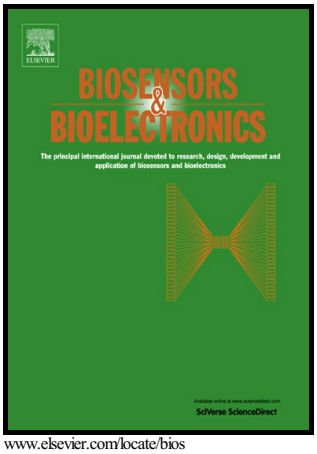

www.elsevier.com/locate/bios

Signal-on fluorescence biosensor for microRNA-21 detection based on DNA strand displacement reaction and Mg^{2+}-dependent DNAzyme cleavage

Huan-Shun Yin, Bing-Chen Li, Yun-Lei Zhou, Hai-Yan Wang, Ming-Hui Wang, Shi-Yun Ai

PII: S0956-5663(17)30308-1
DOI: http://dx.doi.org/10.1016/j.bios.2017.04.049
Reference: BIOS9710

To appear in: *Biosensors and Bioelectronic*

Received date: 6 February 2017
Revised date: 28 April 2017
Accepted date: 28 April 2017

Cite this article as: Huan-Shun Yin, Bing-Chen Li, Yun-Lei Zhou, Hai-Yan Wang, Ming-Hui Wang and Shi-Yun Ai, Signal-on fluorescence biosensor for microRNA-21 detection based on DNA strand displacement reaction and Mg^{2+} dependent DNAzyme cleavage, *Biosensors and Bioelectronic* http://dx.doi.org/10.1016/j.bios.2017.04.049

Signal-on fluorescence biosensor for microRNA-21 detection based on DNA strand displacement reaction and Mg^{2+}-dependent DNAzyme cleavage

Huan-Shun Yin, Bing-Chen Li, Yun-Lei Zhou*, Hai-Yan Wang, Ming-Hui Wang, Shi-Yun Ai*

College of Chemistry and Material Science, Shandong Agricultural University, Taian, 271018, PR China

zhyl@sdau.edu.cn (Yun-Lei Zhou)

ashy@sdau.edu.cn (Shi-Yun Ai).

*Corresponding author.

Abstract

MicroRNAs have been involved into many biological processes and are regarded as disease biomarkers. Simple, rapid, sensitive and selective method for microRNA detection is crucial for early diagnosis and therapy of diseases. In this work, sensitive fluorescence assay was developed for microRNA-21 detection based on DNA polymerase induced strand displacement amplification reaction, Mg^{2+}-dependent DNAzyme catalysis reaction, and magnetic separation. In the presence of target microRNA-21, amounts of trigger DNA could be produced with DNA polymerase induced strand displacement amplification reaction, and the trigger DNA could be further hybridized with signal DNA, which was labeled with biotin and AMCA dye.

After introduction of Mg^{2+}, trigger DNA could form DNAzyme to cleave signal DNA. After magnetic separation, the DNA fragment with AMCA dye could give fluorescence signal, which was related to microRNA-21 concentration. Based on the two efficient signal amplifications, the developed method showed high detection sensitivity with low detection limit of 0.27 fM (3σ). In addition, this fluorescence strategy also possessed excellent detection specificity, and could be applied to analyze microRNA-21 expression level in serum of cancer patient. According to the obtained results, the developed fluorescence method might be a promising detection platform for microRNA-21 quantitative analysis in biomedical research and clinical diagnosis.

Graphical abstract

Keywords: Strand displacement amplification; MicroRNA detection; Fluorescence assay; Mg^{2+}-dependent DNAzyme; Magnetic separation.

1. Introduction

MicroRNAs are a kind of short non-coding RNA molecules, which widely exist in the genomes of plants, animals, and viruses. Due to the critical roles of microRNAs in a variety of biological processes, such as gene expression, cell differentiation, cell apoptosis and metabolism, disease development (Niwa and Slack 2007; Zhao and Srivastava 2007), the sequence-specific microRNAs detection has attracted greatly scientific interests. Aberrant expression of microRNA has been associated with a good deal of diseases, including diabetes, Alzheimer's disease and various cancers (Guay

and Regazzi 2013; Li and Kowdley 2012). For instances, microRNA-21 has been identified to be over-expressed in various cancers, such as gastric cancer, esophagus cancer, prostate cancer, glioblastoma, neuroblastoma, breast cancer and lung cancer (Yao et al. 2009). Therefore, microRNAs have become promising biomarkers for diseases, and the development of simple, fast, reliable, and sensitive detection methods for microRNA biomarkers is crucial for early clinical diagnosis of different diseases.

In view of the importance of microRNA assay, many traditional nucleic acid analysis method, such as northern blotting (Varallyay et al. 2008), quantitative reverse transcription-polymerase chain reaction (qRT-PCR) (Sharbati-Tehrani et al. 2008) and microarray (Fang et al. 2006), have been successfully applied for microRNA detection. However, these techniques require microRNA-labeling, complicated operation process, expensive reagent, and long detection time. These deficiencies stimulated the research interest on the development of simple, fast and sensitive detection method with new signal amplification strategy, such as hybridization chain reaction (HCR) (Jiang et al. 2017; Qian et al. 2015; Rana et al. 2016; Torrente-Rodríguez et al. 2016; Trifonov et al. 2016; Yang et al. 2016a), rolling circle amplification (RCA) (Ali et al. 2014; Li et al. 2016; Russell et al. 2014; Rust et al. 2017; Wu et al. 2015a; Yang et al. 2015a), DNA polymerase induced strand displacement amplification reaction (Chen et al. 2015a; Du et al. 2016; Oishi et al. 2014; Wu et al. 2015b; Zhang et al. 2015), enzymatic in situ production of signal molecule (Katz and Minko 2015; Mailloux et al. 2015; Yang et al. 2015b; Yang et al. 2015c; Yin et al. 2015), etc. Among these signal

amplification strategy, DNA polymerase induced strand displacement amplification reaction attracted greatly interests due to its significant single improvement capability. One microRNA molecule can produce times of secondary DNA molecule under the cyclic processes of hybridization, DNA polymerase induced strand extension, nicking enzyme cleavage, DNA polymerase induced strand displacement and microRNA release, hybridization (Chen et al. 2015a; Yin et al. 2013). When coupled with further signal amplification strategy, or electrochemical or optical labels, this strategy can provide significant signal amplification for achieving the purpose of highly sensitive microRNA detection.

Metal ion-depended DNAzymes, a kind of mimic enzyme, have also attracted great attentions in various detection techniques due to the advantages of high catalytic activity, excellent specificity and good stability (Huang et al. 2015; Lu et al. 2015; Willner et al. 2008). These kinds of DNAzymes also exhibit nucleic acid cleavage activities in the presence of added cofactors of different metal ions. Using these properties, pre-designed nucleic acid sequences can be used to form DNAzyme structures for the amplified detection of metal ions or nucleic acid, such as Pb^{2+} (Yun et al. 2016; Zhang et al. 2016b), Zn^{2+} (Liu et al. 2016), Ni^{2+} (Yang et al. 2016b), Cu^{2+} (Ming et al. 2017), DNA methyltransferase (Song et al. 2017b)and microRNA(Cheng et al. 2016; Wu et al. 2016). In addition, the specific self-cleavage property of metal ion-depended DNAzymes could also be employed as signal amplification unit because the catalytic cleavage reaction could undergo multiple circles to induce the cleavage of substrate DNA (Freage et al. 2014).

In this work, a sensitive fluorescence method was developed for microRNA-21 detection based on the integration of two signal amplification strategies of strand displacement reaction and Mg^{2+}-dependent DNAzyme catalysis reaction, where microRNA-21 was used as trigger to induce the strand displacement amplification reaction. In the presence of Mg^{2+}, the products of strand displacement amplification reaction were used as the DNAzyme to cleave the target DNA labeled with biotin and AMCA dye, which make the target DNA forming two fragments, one containing biotin and the other containing AMCA dye. After magnetic separation by streptavidin functionalized magnetic bead, microRNA-21 could be detected based on the relationship between the fluorescence signal and microRNA concentration. Biotin and AMCA-labeled DNA was used as signal molecule and fluorescence probe. Up to now, many fluorescence probes have been developed in fluorescence assays, such as G−quadruplex-selective iridium(III) complex (Leung et al. 2013), G−quadruplex-crystal violet complex (He et al. 2012), Cy3-labeled capture probe DNA (Chao et al. 2016), *in situ* formed copper nanoparticles (Song et al. 2017a), etc. Though with the disadvantages of low fluorescence quantum yield, short fluorescent lifetime, low Photochemical stability, weak biocompatibility (Resch-Genger et al. 2008), organic fluorescent dye-labeled DNA probe has been widely applied in nucleic detection using fluorescence technique because the easily commercialized synthesis. Thus organic fluorescent dye-labeled DNA probe was employed in this work. Moreover, the developed method was further applied to assay microRNA-21 content in serum samples.

2. Experimental

2.1 Reagents and materials

Nt.BstNBI nicking endonuclease, Taq DNA polymerase, T4 DNA ligase and streptavidin functionalized magnetic bead were purchased from New England Biolabs (USA), where the recognition site for Nt.BstNBI was 5'-GAGTCNNNNN-3', and N represented random oligonucleotide. DNA and deoxyribonucleoside triphosphates (dNTPs, 100 mM) were provided by Sangon (Shanghai, China). microRNA was offered by TAKARA (Dalian, China). The oligonucleotide sequences were listed as follows. DNA-template, 5′- GAT ATC AGC GAT CAC CCA TGT TAC TCT CTA ACA GAC TCT CAA CAT CAG TCT GAT AAG CTA-3′; Signal DNA, 5′-biotin-AGA GTA TrAG GAT ATC-AMCA-3′ (“rA” denotes an A base of RNA.); microRNA-21, 5'-UAG CUU AUC AGA CUG AUG UUG A-3'; microRNA-22, 5′-AAG CUG CCA GUU GAA GAA CUG U-3′; microRNA-141, 5'-UAA CAC UGU CUG GUA AAG AUG G-3'; microRNA-150, 5′-UCU CCC AAC CCU UGU ACC AGU G-3′; microRNA-429, 5'-UAA UAC UGU CUG GUA AAA CCG U-3'. DNA sequences were purified by denaturing polyacrylamide gel electrophoresis, and microRNA sequences were purified by high performance liquid chromatography. Human serum samples were provided by Tai'an City Center Hospital (Shandong, China).

The buffer solutions used in this work are as follows. MicroRNA and DNA dissolve buffer, 10mM Tris-HCl, 1mM EDTA (pH=8.0). Sodium phosphate–sodium chloride buffer solution (SPSC buffer), 0.2 M NaCl, 10 mM Na_2HPO_4, pH 8.0. Thermol buffer,

20 mM Tris-HCl, 10 mM $(NH_4)_2SO_4$, 10 mM KCl, 2 mM $MgSO_4$, 0.1% Triton X-100, pH 8.8. All solutions were prepared with autoclaved 0.1% DEPC water.

2.2 MicroRNA hybridization with DNA template

10 μL of 0.1 μM DNA template and 10 μL of different concentrations of microRNA-21 were added into 10 μL of the buffer solution of 150 mM Tris-HCl, 300 mM NaCl, 30 mM $MgCl_2$, 300 μg/mL BSA (pH 7.9). The mixed solution was heated to 95 ºC for five min to denature DNA template and target microRNA-21. And then, the solution was cooled to 55 ºC naturally and incubated for 1 h to make the complete hybridization of DNA and microRNA. The obtained solution was named as solution A (30 μL).

2.3 Strand displacement amplification

10 μL of 200 unit/mL Nt.BstNBI nicking endonuclease, 10 μL of 180 unit/mL phi29 DNA polymerase，20 μL 4×ThermoPol buffer and 20 μL DEPC-treated sterile water was mixed in 200 μL centrifuge tube. The mixed solution was named as solution B (60 μL). Afterwards, solution A and solution B was mixed and the obtained mixed solution (Marked as solution C, 90 μL) was incubated for 240 min at 55 ºC to generate trigger DNA. The reaction was terminated with incubation at 80 ºC for 20 min.

2.4 DNAzyme digestion

10 μL of 5 nM signal DNA, 10 μL of solution C and 10 μL of 3× SPSC buffer was added into a 500 μL centrifuge tube and mixed homogeneously using vortex. Then, the mixed solution was centrifuged at 4 ºC for 1 min with 10,000 rpm, and the mixed

solution was incubated at 95 ºC for 5 min to complete the hybridization reaction between signal DNA and trigger DNA. After cooled to room temperature, 70 μL of 200 mM $MgCl_2$ solution was added into the above mixed solution and incubated at room temperature for 120 min. After that 10 μL of 0.2 mg/mL streptavidin functionalized magnetic bead was introduced into the reaction solution and incubated at 37 ºC for 45 min. Finally, the magnetic bead was precipitated at the bottom of the centrifuge tube with the aid of magnet, and the supernate was collected for fluorescence detection.

2.5 Fluorescence detection

Fluorescence detection was performed at Cary Eclipse Fluorescence Spectrophotometer (Varian, USA). The AMCA fluorescence dye labeled at the 3'-terminal of DNA was excited at 347 nm, and the fluorescence emission spectra were recorded in the region 390-530 nm. The slit width of 5 nm was used for both excitation and emission. For minimizing the effect of RNase on microRNA detection, all glassware, pipette tips and centrifuge tubes were immersed in 0.1% DEPC (DEPC-water) for 24 h, then they were autoclaved and dried at 60 ºC for 12 h.

2.6 Total RNA extraction from human serum

Total RNA was extracted from human serums with miRNeasy Serum/Plasma Kit (Qiagen, GER) according to the manufacturer's instructions and stored at -80 ºC before detection. The integrity of the extracted total RNA was characterized by 0.8% agarose gel electrophoresis, which was carried out on a DYCP-31DN electrophoresis apparatus (Beijing Liuyi Instrument Factory, Beijing, China). The concentration of the

total RNA was detected by Quawell Q5000 micro-volume UV-Vis spectrophotometer (USA).

3. Results and discussion

3.1 Detection strategy

In this work, a signal-on fluorescence method was developed for microRNA-21 detection based on DNA polymerase and nicking enzyme triggered strand displacement amplification and Mg^{2+}-dependent DNAzyme induced fluorescence improvement. The detection process was illustrated in Scheme 1. Firstly, a linear DNA template was designed containing three regions: microRNA-21 hybridization region, Nt.BstNBI nicking endonuclease recognition region, and DNA strand amplification region. In addition, another linear DNA labeled with biotin at its 5'-terminal and AMCA at its 3'-terminal (named as signal DNA) was employed, which can hybridized with trigger DNA, and cleaved by DNAzyme in the presence of Mg^{2+}. As shown in section A of Scheme 1, after microRNA-21 hybridized with linear template DNA, the target microRNA-21 can be extend along the linear DNA template to its 5'-terminal and form a duplex structure in the presence of DNA polymerase and dNTPs. Afterwards, Nt.BstNBI nicking endonuclease can recognize the nicking site and generate a gap at the upper strand, which can also trigger a new round replication catalyzed by DNA polymerase and the first replicated DNA strand can be displaced and released. As a result, a mass of trigger DNA can be produced based on the repetitive strand extension, nicking and strand displacement reaction. The released trigger DNA can hybridize with signal DNA partly to from DNAzyme in the presence

of Mg^{2+}, which can result in the cleavage of signal DNA to from two fragments, one contains biotin and another contains AMCA dye. Subsequently, streptavidin functionalized magnetic bead can bind with biotin modified DNA fragment or signal DNA, and this complex can be precipitated to the bottom of the centrifuge tube with the aid of magnet. The DNA fragment containing AMCA dye will remain in the supernate. After separation, a fluorescence signal can obtained and the signal intensity is related to the concentration of target microRNA-21. Therefore, this strategy can be applied to detect microRNA-21.

3.2 Detection feasibility assay

To verify the detection feasibility of the developed method for microRNA-21 assay, several experiments were carried out based on the experiment processes as described in Experimental section except that some experiment conditions were changed. The fluorescence response was recorded in the range from 390 to 430 nm and the results were shown in Fig. 1. Curve a was the fluorescence response of the developed method except signal DNA. It was clear that no fluorescence response was obtained in the selected wavelength range, indicating that no fluorescence molecule was introduced in the detection system, which was in accord with the fact of the absence of signal DNA labeled with AMCA. Curve b was the fluorescence response without target microRNA-21, and almost no fluorescence signal was observed. Without target microRNA-21, the strand displacement amplification reaction cannot be performed, which led to more signal DNA precipitated at the bottom of centrifuge tube in the presence of magnetic bead. When signal DNA and target microRNA-21 (1 fM) were

both introduced into the detection system (that is to say, the detection process was performed as described in Experimental section), a strong fluorescence signal was observed (curve c), which was higher that of curve b. In the presence of target microRNA-21 more trigger DNA were produced due to the strand displacement amplification reaction under the aid of Nt.BstNBI nicking endonuclease and DNA polymerase, which led to more signal DNA cleaved by Mg^{2+}-dependent DNAzyme. As a result, more signal DNA fragments labeled with AMCA were remained in the supernate to emit strong fluorescence signal. When microRNA-21 concentration increased from 1 to 100 fM and 10 pM, respectively, the fluorescence response increased significantly (curve d and curve e). With increasing microRNA-21 concentration, more trigger DNA can be generated under the same conditions, and more signal DNA can be cleaved by the Mg^{2+}-dependent DNAzyme. Consequence, only little signal DNA fragment labeled with AMCA and biotin can be precipitated based on the interaction between biotin and strepavidin functionalized magnetic bead, and more AMCA still remained in the supernate. According to difference fluorescence response caused by microRNA-21 concentration variation, we think that the developed method can be applied to detect microRNA-21.

In the developed detection strategy, two kinds of signal amplification patterns were employed, strand displacement amplification and Mg^{2+}-dependent DNAzyme catalysis signal amplification. In the two amplification patterns, Nt.BstNBI nicking endonuclease and Mg^{2+} play important functions. Therefore, we investigated the fluorescence response without Nt.BstNBI nicking endonuclease and Mg^{2+},

respectively. As seen in Fig. 1, almost no obvious fluorescence responses were obtained for the absence of Nt.BstNBI nicking endonuclease (curve f) and Mg^{2+} (curve g), respectively. It can be explained as the fact that almost all signal DNA molecules bonded with strepavidin functionalized magnetic bend and precipitated at the bottom of centrifuge tube due to the lack of Mg^{2+}-dependent DNAzyme. Without Nt.BstNBI nicking endonuclease, the strand displacement reaction cannot achieve and the produced double strands DNA cannot further hybridize with signal DNA, which resulted in the failure of the formation of Mg^{2+}-dependent DNAzyme. These results demonstrated that the activity of Nt.BstNBI nicking endonuclease and the content of Mg^{2+} can greatly influence microRNA-21 detection.

In addition, the influence of strepavidin functionalized magnetic bend was also investigated. As shown in Fig. 1, a strong fluorescence signal was obtained without strepavidin functionalized magnetic bend (curve h). Though the generated Mg^{2+}-dependent DNAzyme cleaved the signal DNA to form two fragments, all the fragments labeled with AMCA remained in the supernate due to the lack of strepavidin functionalized magnetic bend.

Based on the above investigations, we think that the developed method can be applied to detect microRNA-21 with high sensitivity.

3.4 Optimization of detection conditions

To achieve high detection sensitivity, several experimental parameters were optimized, such as Nt.BstNBI nicking endonuclease concentration, DNA polymerase concentration, strand displacement reaction time, Mg^{2+} concentration, DNAzyme

reaction time, avidin-biotin reaction time.

In this detection strategy, strand displacement amplification plays crucial action for high sensitivity detection of microRNA-21. Therefore, in this process three factors (DNA polymerase concentration, Nt.BstNBI nicking endonuclease concentration and strand displacement reaction time) were optimized. Fig. 2A presented the influence of DNA polymerase concentration on fluorescence response of AMCA dye. With increasing DNA polymerase concentration from 30 to 180 unit/mL, the fluorescence intensity increased gradually. When furthering enhancing DNA polymerase concentration, the fluorescence intensity tended to level off. Therefore, 180 unit/mL was selected as the optimal concentration. The effect of Nt.BstNBI nicking endonuclease concentration on AMCA fluorescence response was also investigated, and the results were also illustrated in Fig. 2A. When the concentration of Nt.BstNBI varied from 25 to 200 unit/mL, the fluorescence intensity improved correspondingly, and the optimum concentration was obtained at 200 unit/mL. Thus, this concentration was used throughout the experiment.

The impact of strand displacement reaction time on microRNA-21 detection was illustrated in Fig. 2B. With extending the reaction time form 30 to 240 min, the fluorescence intensity increased quickly. Then, a plateau was achieved when further prolonging the reaction time to 360 min. considering the detection efficiency, 360 min was chosen. DNAzyme reaction time was also optimized and the result was shown in Fig. 2B. 120 min was chosen as the optimal experiment condition.

The second signal amplification is mainly depended on the activity of DNAzyme,

and the latter is depended on Mg^{2+}, so the concentration of Mg^{2+} was optimized. As shown in Fig. 2C, the fluorescence intensity increased gradually with changing Mg^{2+} concentration form 10 to 200 mM, and then the fluorescence response tended to level off. Therefore, 200 mM was used. Furthermore, the capture time for magnetic bead towards signal DNA was also investigated. For performing it, 20 μL signal DNA and 20 μL magnetic bead were added into 500 μL centrifuge tube, and mixed with vortex shaking. After different time incubation, the supernate was collected with magnetic separation. As shown in Fig. 2D, with extending the capture time to 45 min, the fluorescence intensity decreased gradually. And when the capture time was high than 45 min, the fluorescence response tended to level off, indicating that almost all signal DNA was captured by magnetic bead and participated at the bottom of centrifuge tube. Consequently, 45 min was used as the optimal capture time.

3.5 Detection performances

Under optimal experiment conditions, the detection performances of the developed method for microRNA-21 were investigated. Fig. 3A illustrated the relationship between fluorescence response and microRNA-21 concentration. With increasing microRNA-21 concentration from 1 fM to 50 pM, the fluorescence response enhanced gradually. A linear relationship can be obtained between fluorescence response and the logarithm value of microRNA-21 concentration (Fig. 3B). The linear regression equation was expressed as $F = 108.22\log c + 197.33$ (R=0.9954), and the limit of detection (LOD) was calculated to be 0.27 fM (3σ). The detection performances of the developed method were compared with some of previous reports on microRNA

detection using different methods, and the results were listed in Table 1. The LOD and linear range of this work was comparable with some of previous work.

The detection specificity of the developed method was evaluated using 5 pM of different microRNAs as detection target, such as complementary microRNA (microRNA-21), microRNA-22, microRNA-141, microRNA-150 and microRNA-429. The fluorescence intensity for different microRNAs was compared. As shown in Fig. 3C, the fluorescence intensity for microRNA-21 was greatly higher than that obtained at other four microRNAs, indicating that the developed method can excellent discriminate target microRNA-21 and other three microRNAs. It could be ascribed to the fact that the non-complementary microRNA could not hybridize with template DNA with high efficiency, which led to the low amount of Mg^{2+}-dependent DNAzyme. This result also demonstrated that the developed method possessed good detection specificity.

As a kind of significant factor to estimate a method used for practical application, the reproducibility of the developed fluorescence method was tested according to the relative standard deviation (RSD), which was obtained by detect 0.1 pM target microRNA-21 for 10 times with the same process as described in Experimental section. As seen in Fig. 3D, a RSD of 3.43% was achieved, indicating that the proposed detection strategy shared acceptable reproducibility.

3.6 Sample assay

To testify the applicability of the developed strategy for microRNA detection in real samples, the expression levels of microRNA-21 in gastric cancer patient serum and

healthy human serum were detected and compared. For avoiding the interference of DNA with same sequence of microRNA-21, the total RNA was extracted from the sample without DNA. As shown in Fig. 4, the expression level of microRNA-21 in gastric cancer patient serum was higher than that at healthy human serum, indicating that microRNA-21 might be a kind of biomarker for gastric cancer. For proving the detection veracity, the expression level of microRNA-21 was also detected by qRT-PCR and the results were also listed in Fig. 4. The results obtained by qRT-PCR were similar to that by the developed method of this work, indicating the proposed fluorescence detection strategy had good veracity.

4. Conclusions

In summary, a sensitive fluorescence method was developed for microRNA-21 detection based on the strand displacement amplification reaction and Mg^{2+}-dependent DNAzyme catalytic signal amplification. Under the cyclic process of microRNA-21 hybridization, DNA polymerase inducing strand extension, nicking enzyme cleavage, and strand displacement reaction, low number of target microRNA-21 can generate times of trigger DNA to form Mg^{2+}-dependent DNAzyme, which can greatly improve the fluorescence signal after magnetic separation. The developed method is simple and easy-operated with high detection sensitivity and specificity accompanied with the disadvantage of dye label. In addition, the high expression level of microRNA-21 in cancer patient serum was also confirmed. Thus the developed fluorescence method might be a promising detection platform for microRNA-21 detection in clinical diagnostics and biochemical researches.

Acknowledgements

This work was supported by the Natural Science Foundation of Shandong province, China (No. ZR2014BQ029) and the National Natural Science Foundation of China (No. 21375079).

References

Ali, M.M., Li, F., Zhang, Z., Zhang, K., Kang, D.-K., Ankrum, J.A., Le, X.C., Zhao, W., 2014. Chem. Soc. Rev. 43, 3324-3341.

Cao, H., Liu, S., Tu, W., Bao, J., Dai, Z., 2014. Chem. Commun. 50, 13315-13318.

Chao, J., Li, Z., Li, J., Peng, H., Su, S., Li, Q., Zhu, C., Zuo, X., Song, S., Wang, L., Wang, L., 2016. Biosens Bioelectron 81, 92-96.

Chen, A., Gui, G.-F., Zhuo, Y., Chai, Y.-Q., Xiang, Y., Yuan, R., 2015a. Anal. Chem. 87, 6328-6334.

Chen, A., Ma, S., Zhuo, Y., Chai, Y., Yuan, R., 2016. Anal. Chem. 88, 3203-3210.

Chen, Y., Xiang, Y., Yuan, R., Chai, Y., 2015b. Anal. Chim. Acta 891, 130-135.

Cheng, F.-F., Jiang, N., Li, X., Zhang, L., Hu, L., Chen, X., Jiang, L.-P., Abdel-Halim, E.S., Zhu, J.-J., 2016. Biosens. Bioelectron. 85, 891-896.

Chi, B.-Z., Liang, R.-P., Qiu, W.-B., Yuan, Y.-H., Qiu, J.-D., 2017. Biosens. Bioelectron. 87, 216-221.

Du, Y.-C., Zhu, L.-N., Kong, D.-M., 2016. Biosens. Bioelectron. 86, 811-817.

Fang, S., Lee, H., Wark, A., Corn, R., 2006. J. Am. Chem. Soc. 128, 14044-14046.

Feng, Q.-M., Shen, Y.-Z., Li, M.-X., Zhang, Z.-L., Zhao, W., Xu, J.-J., Chen, H.-Y., 2016. Anal. Chem. 88, 937-944.

Freage, L., Wang, F., Orbach, R., Willner, I., 2014. Anal. Chem. 86, 11326-11333.

Guay, C., Regazzi, R., 2013. Nat. Rev. Endocrinol. 9, 513-521.

He, H.-Z., Pui-Yan Ma, V., Leung, K.-H., Shiu-Hin Chan, D., Yang, H., Cheng, Z., Leung, C.-H., Ma, D.-L., 2012. Analyst 137, 1538-1540.

Huang, Y., Lei, J., Cheng, Y., Ju, H., 2015. Electrochim. Acta 155, 341-347.

Jiang, B., Wei, Y., Xu, J., Yuan, R., Xiang, Y., 2017. Anal. Chim. Acta 949, 83-88.

Katz, E., Minko, S., 2015. Chem. Commun. 51, 3493-3500.

Leung, K.-H., He, H.-Z., Wang, W., Zhong, H.-J., Chan, D.S.-H., Leung, C.-H., Ma, D.-L., 2013. ACS Appl Mater Interfaces 5, 12249-12253.

Li, B., Li, X., Wang, M., Yang, Z., Yin, H., Ai, S., 2015. J. Solid State Electrochem. 19, 1301-1309.

Li, X., Guo, J., Zhai, Q., Xia, J., Yi, G., 2016. Anal. Chim. Acta 934, 52-58.

Li, Y., Kowdley, K.V., 2012. Genomics, Proteomics Bioinf. 10, 246-253.

Liu, N., Hou, R., Gao, P., Lou, X., Xia, F., 2016. Analyst 141, 3626-3629.

Lu, L., Si, J.C., Gao, Z.F., Zhang, Y., Lei, J.L., Luo, H.Q., Li, N.B., 2015. Biosens. Bioelectron. 63, 14-20.

Lv, W., Zhao, J., Situ, B., Li, B., Ma, W., Liu, J., Wu, Z., Wang, W., Yan, X., Zheng, L., 2016. Biosens. Bioelectron. 83, 250-255.

Ma, W., Situ, B., Lv, W., Li, B., Yin, X., Vadgama, P., Zheng, L., Wang, W., 2016. Biosens. Bioelectron. 80, 344-351.

Mailloux, S., Gerasimova, Y.V., Guz, N., Kolpashchikov, D.M., Katz, E., 2015. Angew. Chem. Int. Ed. 54, 6562-6566.

Ming, J., Fan, W., Jiang, T.-F., Wang, Y.-H., Lv, Z.-H., 2017. Sens. Actuators, B-Chem. 240, 1091-1098.

Niu, C., Song, Q., He, G., Na, N., Ouyang, J., 2016. Anal. Chem. 88, 11062-11069.

Niwa, R., Slack, F.J., 2007. Curr. Opin. Genet. Dev. 17, 145-150.

Oishi, M., Nakao, S., Kato, D., 2014. Chem. Commun. 50, 991-993.

Pang, X., Qi, J., Zhang, Y., Ren, Y., Su, M., Jia, B., Wang, Y., Wei, Q., Du, B., 2016. Biosens. Bioelectron. 85, 142-150.

Qian, Y., Wang, C., Gao, F., 2015. Biosens. Bioelectron. 63, 425-431.

Rafiee-Pour, H.-A., Behpour, M., Keshavarz, M., 2016. Biosens. Bioelectron. 77, 202-207.

Rana, M., Balcioglu, M., Kovach, M., Hizir, M.S., Robertson, N.M., Khan, I., Yigit, M.V., 2016. Chem. Commun. 52, 3524-3527.

Resch-Genger, U., Grabolle, M., Cavaliere-Jaricot, S., Nitschke, R., Nann, T., 2008. Nature Methods 5, 763-775.

Russell, C., Welch, K., Jarvius, J., Cai, Y., Brucas, R., Nikolajeff, F., Svedlindh, P., Nilsson, M., 2014. ACS nano 8, 1147-1153.

Rust, P., Cereghetti, D., Dual, J., 2017. Sens. Actuators, B-Chem. 239, 1118-1123.

Sharbati-Tehrani, S., Kutz-Lohroff, B., Bergbauer, R., Scholven, J., Einspanier, R., 2008. BMC Mol. Biol. 9, 34.

Shi, K., Dou, B., Yang, C., Chai, Y., Yuan, R., Xiang, Y., 2015. Anal. Chem. 87, 8578-8583.

Song, Q., Wang, R., Sun, F., Chen, H., Wang, Z., Na, N., Ouyang, J., 2017a. Biosens

Bioelectron 87, 760-763.

Song, W., Luan, Y., Guo, X., He, P., Zhang, X., 2017b. Anal. Chim. Acta 956, 57-62.

Torrente-Rodríguez, R.M., Campuzano, S., Montiel, V.R.-V., Montoya, J.J., Pingarróna, J.M., 2016. Biosens. Bioelectron. 86, 516-521.

Trifonov, A., Sharon, E., Tel-Vered, R., Kahn, J.S., Willner, I., 2016. J. Phys. Chem. C 120, 15743-15752.

Tu, W., Cao, H., Zhang, L., Bao, J., Liu, X., Dai, Z., 2016. Anal. Chem. 88, 10459-10465.

Varallyay, E., Burgyan, J., Havelda, Z., 2008. Nat. Protoc. 3, 190-196.

Willner, I., Shlyahovsky, B., Zayats, M., Willner, B., 2008. Chem. Soc. Rev. 37, 1153-1165.

Wu, L., Ma, C., Zheng, X., Liu, H., Yu, J., 2015a. Biosens. Bioelectron. 68, 413-420.

Wu, W., Mao, Y., Zhao, S., Lu, X., Liang, X., Zeng, L., 2015b. Anal. Chim. Acta 881, 124-130.

Wu, X., Chai, Y., Yuan, R., Zhuo, Y., Chen, Y., 2014. Sens. Actuators, B-Chem. 203, 296-302.

Wu, Y., Sheng, K., Liu, Y., Yu, Q., Ye, B., 2016. Anal. Chim. Acta 948, 1-8.

Xi, Q., Zhou, D.-M., Kan, Y.-Y., Ge, J., Wu, Z.-K., Yu, R.-Q., Jiang, J.-H., 2014. Anal. Chem. 86, 1361-1365.

Yang, L., Zhang, Y., Li, R., Lin, C., Guo, L., Qiu, B., Lin, Z., Chen, G., 2015a. Biosens. Bioelectron. 70, 268-274.

Yang, Y., Liu, X., Wu, M., Wang, X., Hou, T., Li, F., 2016a. Sens. Actuators, B-Chem.

236, 597-604.

Yang, Y., Yuan, Z., Liu, X.-P., Liu, Q., Mao, C.-J., Niu, H.-L., Jin, B.-K., Zhang, S.-Y., 2016b. Biosens. Bioelectron. 77, 13-18.

Yang, Z.-H., Zhuo, Y., Yuan, R., Chai, Y.-Q., 2015b. Biosens. Bioelectron. 69, 321-327.

Yang, Z., Wang, F., Wang, M., Yin, H., Ai, S., 2015c. Biosens. Bioelectron. 66, 109-114.

Yao, Q., Xu, H., Zhang, Q.-Q., Zhou, H., Qu, L.-H., 2009. Biochem. Biophys. Res. Commun. 388, 539-542.

Yin, B.-C., Liu, Y.-Q., Ye, B.-C., 2013. Anal. Chem. 85, 11487-11493.

Yin, H., Sun, B., Dong, L., Li, B., Zhou, Y., Ai, S., 2015. Biosens. Bioelectron. 64, 462-468.

Yin, H., Zhou, Y., Li, B., Li, X., Yang, Z., Ai, S., Zhang, X., 2016. Sens. Actuators, B-Chem. 222, 1119-1126.

Yu, Y.-Q., Wang, J.-P., Zhao, M., Hong, L.-R., Chai, Y.-Q., Yuan, R., Zhuo, Y., 2016. Biosens. Bioelectron. 77, 442-450.

Yun, W., Cai, D., Jiang, J., Zhao, P., Huang, Y., Sang, G., 2016. Biosens. Bioelectron. 80, 187-193.

Zhang, H., Li, F., Chen, H., Ma, Y., Qi, S., Chen, X., Zhou, L., 2015. Sens. Actuators, B-Chem. 207, Part A, 748-755.

Zhang, T., Zhao, H., Fan, G., Li, Y., Li, L., Quan, X., 2016a. Electrochim. Acta 190, 1150-1158.

Zhang, Y., Xiao, S., Li, H., Liu, H., Pang, P., Wang, H., Wu, Z., Yang, W., 2016b. Sens. Actuators, B-Chem. 222, 1083-1089.

Zhao, Y., Srivastava, D., 2007. Trends Biochem. Sci. 32, 189-197.

Figure captions

Scheme 1. Schematic illustration of biosensor fabrication and electrochemical detection of microRNA.

Fig. 1. Fluorescence responses of AMCA under different assay conditions. (a) Without signal DNA. (b) Without target microRNA-21. (c) MicroRNA-21 concentration was 1 fM. (d) MicroRNA-21 concentration was 100 fM. (e) MicroRNA-21 concentration was 10 pM. (f) Without Nt.BstNBI nicking endonuclease. (g) Without Mg^{2+}. (h) Without streptavidin functionalized magnetic bead.

Fig. 2. The effect of Nt.BstNBI nicking endonuclease concentration (■) and DNA polymerase concentration (◆) (A), strand displacement reaction time (■) and DNAzyme reaction time (◆) (B), Mg^{2+} concentration (C), and avidin-biotin reaction time (D) on fluorescence response of AMCA.

Fig. 3. (A) Fluorescence response of the biosensor for different concentrations of microRNA-21. a-k, 1, 5, 10, 50, 100, 500, 1000, 5000, 10000, 50000 fM (B) The

linear relationship between the fluorescence change and microRNA-21 concentration. (C) The histogram of the fluorescence change for 5 pM of different microRNAs. (D) The histogram for fluorescence response of 0.1 pM microRNA-21 obtained at 10 biosensors fabricated dependently.

Fig. 4. The histogram for microRNA-21 expression level in healthy human serum (a) and gastric cancer patient serum (b).

Table 1. The comparison of detection performances of the developed method with other methods.

Methods	Target MicroRNA	Linear range (M)	LOD (fM)	Refs
Electrochemistry	miRNA-21	10^{-14}-10^{-8}	9	(Ma et al. 2016)
Electrochemistry	miRNA-21	10^{-13}-5×10^{-10}	84.3	(Rafiee-Pour et al. 2016)
Electrochemistry	miRNA-155	10^{-14}-10^{-9}	3.3	(Wu et al. 2014)
Electrochemistry	miRNA-21	5×10^{-15}-5×10^{-10}	1.4	(Shi et al. 2015)
Fluorescence	miRNA-141	10^{-15}-10^{-8}	1	(Yin et al. 2013)
Fluorescence	miRNA-21	10^{-12}-10^{-9}	100	(Chi et al. 2017)
Fluorescence	miRNA-21	10^{-14}-10^{-11}	7.3	(Lv et al. 2016)
Fluorescence	miRNA-21	10^{-12}-10^{-8}	300	(Xi et al. 2014)
Fluorescence	let-7d	10^{-11}-10^{-10}	8400	(Niu et al. 2016)
Photoelectrochemistry	miRNA-319a	5×10^{-15}-3×10^{-12}	2.26	(Yin et al. 2016)
Photoelectrochemistry	miRNA-155	10^{-17}-2×10^{-8}	0.005	(Pang et al. 2016)
Photoelectrochemistry	miRNA-21	10^{-15}-5×10^{-13}	0.56	(Li et al. 2015)
Photoelectrochemistry	miRNA-7f	5×10^{-14}-10^{-10}	34	(Cao et al. 2014)
Photoelectrochemistry	miRNA-122a	3.5×10^{-13}-5×10^{-9}	153	(Tu et al. 2016)
ECL	miRNA-21	10^{-15}-10^{-9}	0.5	(Feng et al. 2016)
ECL	miRNA-20a	10^{-13}-10^{-8}	100	(Zhang et al. 2016a)
ECL	miRNA-141	10^{-14}-1.2×10^{-12}	5.5	(Chen et al. 2015b)
ECL	miRNA-21	10^{-16}-10^{-11}	0.03	(Yu et al. 2016)
ECL	miRNA-21	10^{-16}-10^{-11}	0.022	(Chen et al. 2016)
Fluorescence	miRNA-21	10^{-15}-5×10^{-11}	0.27	This work

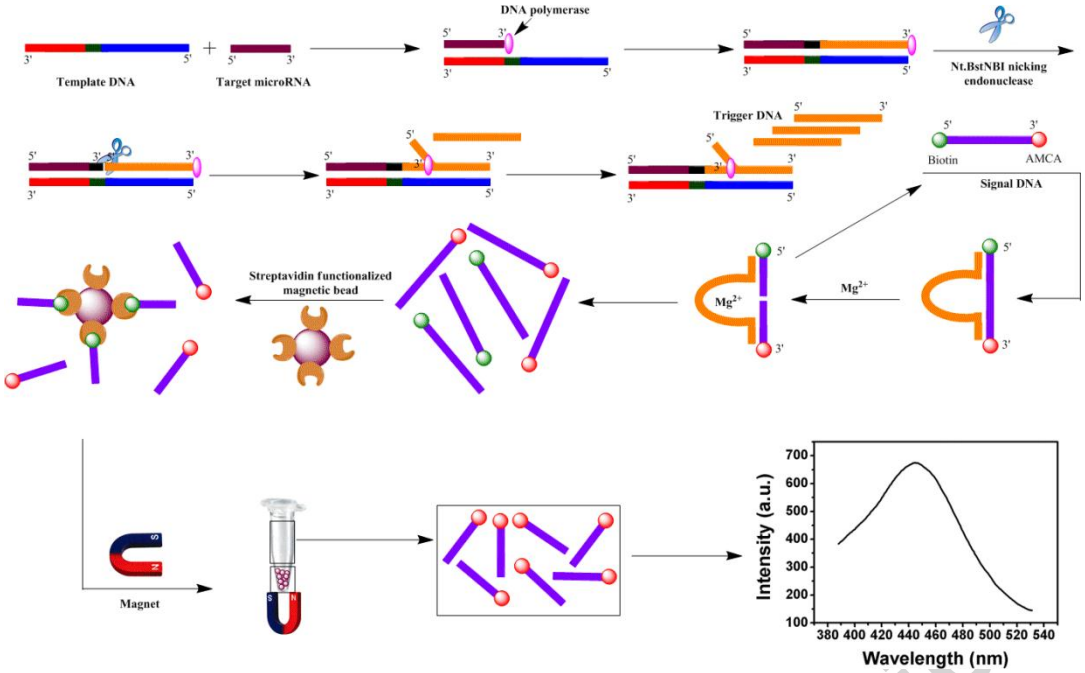

Highlights

- A sensitive fluorescence biosensor was fabricated for miRNA-21 detection.
- DNA strand displacement reaction and Mg^{2+}-dependent DNAzyme cleavage strategy was employed.
- The developed method showed wide linear range from 1 fM to 50 pM and low detection limit of 0.27 fM.
- This method can be applied to analysis the expression level of miRNA-21 in gastric cancer cell.